

The effects of optical fiber impairments on communication systems

Riyam Saadi Ali, Ali Y. Fattah, Mustafa D. Hassib

Department of Communication Engineering, University of Technology, Baghdad, Iraq

Article Info

Article history:

Received Mar 10, 2022

Revised Jun 24, 2022

Accepted Jul 14, 2022

Keywords:

Characterization

Fiber optics

Optical Gaussian pulse

Optisystem

Physical layer impairments

ABSTRACT

In this paper, the influence of physical layer impairments on fiber optic channels was evaluated using analytical modeling, and the findings were verified through simulation results. Light propagation inside standard single mode fiber (SSMF) is affected by both linear and nonlinear effects, which must be taken into account in order to develop an appropriate fiber channel model. The use of nonlinear fiber optics in the implementation of high-capacity optical networks is crucial. The "Optisystem 17.0" software package was used to simulate the suggested systems. It can be observed that increased input power tends to increase the effect of cross-phase modulation (XPM) and four wave mixing (FWM) in the nonlinear dispersive fibers. The impact of pulse broadening due to chromatic dispersion (CD), self-phase modulation (SPM), and cross-phase modulation (XPM) was investigated using Gaussian pulses as input signals.

This is an open access article under the [CC BY-SA](https://creativecommons.org/licenses/by-sa/4.0/) license.



Corresponding Author:

Riyam Saadi Ali

Department of Communication Engineering, University of Technology

Baghdad, Iraq

Email: coe.20.02@grad.uotechnology.edu.iq

1. INTRODUCTION

Communication systems are the means by which information is transferred from one site to another. Information is commonly transferred by superimposing as well as modulating it on an electromagnetic wave that serves as a carrier for the message signal. This modulated carrier can then be transmitted to the appropriate location, where it is received and demodulated to recover the original message signal. Radio, microwave, millimeter wave, and optical frequencies are all possible for electromagnetic carrier waves. Carriers with frequencies in the visible or near-infrared range of the electromagnetic spectrum are used in optical fiber communication, also known as lightwave systems. Fiber optic communication networks are lightwave communication systems in which data is sent through an optical fiber [1]. Wavelength division multiplexing (WDM) enables each fiber to transfer multiple independent channels at different wavelengths of light. The WDM system was developed by the International Telecommunication Union (ITU) [2]. Numerous distortion mechanisms, including nonlinear effects and signal dispersion factors, restrict the information-carrying capacity. For high-performance SMF, the two main types of distortion are chromatic as well as polarization mode dispersions, which results in the broadening of optical signal pulses even though they travel across a fiber. When there are high power densities in a fiber, nonlinear effects are observed. Their effect on signal fidelity involves power shifts between wavelength channels, the presence of spurious signals at other wavelengths, and signal quality decreases. These nonlinear effects could be particularly problematic in high-rate WDM networks [3]. Linear and nonlinear degradation effects limit the capacity of optical networks. Chromatic dispersion (CD), polarization mode dispersion (PMD), and attenuation are linear degrading effects, whereas nonlinear degrading effects comprise four-wave mixing (FWM), self-phase

modulation (SPM), cross-phase modulation (XPM), stimulated raman scattering (SRS), and stimulated brillouin scattering (SBS) [4]. A linear medium is one in which the optical power confined within the fiber is low. In this situation, the attenuation and refractive index of the fiber may be determined regardless of input power. However, when the input power increases, the medium's nonlinearity impacts become more apparent [5]. A key parameter in lightwave systems is the bandwidth-distance product. Increased data rate for each channel and narrower channel spacing in dense wavelength division multiplexed (DWDM) systems are two types of techniques for increasing the capacity of lightwave systems. A 40 Gb/s or higher data-rate DWDM system is unavoidable in next-generation lightwave systems. Linear and nonlinear impairments get much worse in these kinds of high-speed DWDM systems [6].

Several approaches for increasing the productivity of WDM transmission networks have been presented, including carving envelopes to shape envelopes of phase conjugated dual subcarriers lowers induced nonlinear phase noise [7]. Optical phase conjugation (OPC) is an efficient strategy for compensating for deterministic impairments, including Kerr nonlinearities, CD and PMD, in long-distance transmission systems. Impairments that occurred in the first portion of the transmission link (before conjugation) could be cancelled by impairments that occur in the second portion of the link by optically conjugating the phase of the signal in the middle of the link (after conjugation) [8], [9]. When compared to intensity modulation formats, phase modulation formats have numerous advantages. Differential phase-shift keying (DPSK) and, in particular, differential quadrature phase-shift keying (DQPSK) enhance, among other things, the Bit Error Rate and communication reach. Polarization division multiplexing quadrature phase-shift keying (PDM-QPSK) is a promising option that improves spectral efficiency, optical signal to noise (OSNR) ratio, and CD tolerances [10]. Higher modulation formats (RZ-4QAM and RZ-16QAM) have been suggested to improve the efficiency of an all-optical OFDM system [11]. Equally spaced (ES) channels in WDM systems contain a large number of FWM lights whose frequencies correspond to signal lights. As a result, FWM significantly reduces the signal-to-noise (SNR) ratio for ES channels. On the other hand, unevenly spaced (US) channels do not have any FWM lights whose frequency components match with signal lights [12]. For the various modulation formats, the polarization interleaving mechanism is employed to minimize crosstalk between neighboring channels and nonlinear effects. The odd and even numbers of channels are aggregated into two distinct branches, each with orthogonal states of polarization (SOPs) adapted by polarization controllers [13]. The propagation of a pulse in a fiber optic link is characterized by the nonlinear Schrödinger equation, which can be used to understand linear and nonlinear impairments:

$$\frac{\partial A}{\partial z} + \frac{\alpha}{2} A + \beta_1 \frac{\partial A}{\partial t} + \frac{j}{2} \beta_2 \frac{\partial^2 A}{\partial t^2} - \frac{1}{6} \beta_3 \frac{\partial^3 A}{\partial t^3} = j\gamma |A|^2 A \quad (1)$$

where A the optical field magnitude, α attenuation parameter, z the distance of the fiber transmission, β_1 is related to the group velocity, β_2 indicates dispersion of the group velocity, and therefore is responsible for pulse broadening, β_3 is the third-order dispersion coefficient, and γ is the fiber nonlinearity coefficient [14].

In this paper, linear and nonlinear impairments of optical fiber transmission were characterized using analytical modeling and validated using simulation results. Linear effects have been shown to be deterministic and to have a manageable influence on transmission link behavior. Nonlinear impairments, on the other hand, have a nondeterministic and partly manageable influence on the quality of transmission (QoT) of fiber optic data transmission.

2. THEORETICAL BACKGROUND

2.1. Linear impairments

Optical fiber is frequently regarded as the desirable transmission channel, with virtually limitless bandwidth. However, the linear effect of fibers, which is dispersion and attenuation, will become the significant limiting factor as length is increased for multi-span amplified systems and higher bit rates [15]. The linear schrödinger equation (LSE) effectively identifies linear impairments in transmission links. In this case, the propagation constant (β) is first expanded into a Taylor series around the carrier frequency, with only the first three parts in the series expansion. The LSE can be characterized in this way [16]:

$$\frac{\partial A}{\partial z} + \frac{\alpha}{2} A + \beta_1 \frac{\partial A}{\partial t} + \frac{j}{2} \beta_2 \frac{\partial^2 A}{\partial t^2} - \frac{1}{6} \beta_3 \frac{\partial^3 A}{\partial t^3} = 0 \quad (2)$$

2.1.1. Attenuation

The signal power drops exponentially across the transmission line according to fiber loss, the attenuation coefficient is commonly stated as [dB/km]:

$$\alpha_{dB} = \frac{10}{\ln 10} \alpha \approx 4.343\alpha = -\frac{10}{z} \cdot \log \left(\frac{P(z)}{P_{in}} \right) \tag{3}$$

where P_{in} denotes the optical power lunched into a fiber in watt, $P(z)$ denotes the optical power at point z in Watt, z indicates the transmission distance in kilometers and α is the attenuation parameter in neper per kilometer [Np/Km] [17]. Material absorption and Rayleigh scattering are the major causes of attenuation. 1550 nm is the most frequently used wavelength for long-distance optical communications because it has the lowest attenuation as shown in Figure 1 [18].

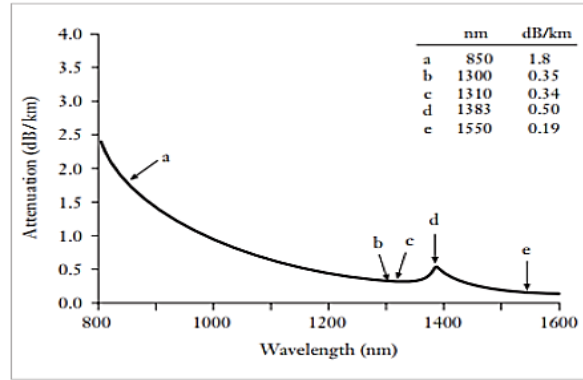


Figure 1. Attenuation profile for standard single-mode fiber [18]

2.1.2. Amplified spontaneous emission noise

An amplified spontaneous emission (ASE) is caused by holes and electrons spontaneously recombining in the amplifier medium. As shown in Figure 2, the ASE noise is increased by the signal during transmission due to a nonlinear interaction between the signal and the ASE noise from optical amplifiers. When numerous optical amplifiers are used to compensate for fiber loss, this is known as cascading, ASE accumulates in the system. The noise created by the preceding amplifiers is amplified by each following amplifier in the cascade [1].

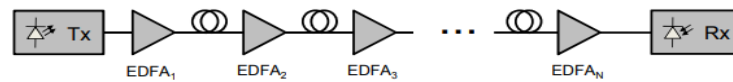


Figure 2. A diagram of an optical transmission link employing EDFAs compensating for fiber loss [19]

Considering that the total loss of the previous span is perfectly compensated by the subsequent EDFA ($Gain = \alpha L_{span}$), the total noise figure NF_{Link} of transmission systems with N spans and periodic EDFA amplification may be described as follows [20]:

$$NF_{Link} = 1 + N(\alpha L_{span} \cdot NF - 1) \tag{4}$$

2.1.3. Chromatic dispersion

The optical pulses move down the fiber at various speeds for different wavelengths, resulting in CD. The difference in speed is produced by the refractive index of the fiber changing with wavelength. Wavelength signal components, causing the optical pulse to broaden as seen in Figure 3. Differential group delay caused by CD in single mode fiber can cause overlapping of high-speed pulses, resulting in ISI and therefore data recovery error [19].



Figure 3. Pulse broadening caused by chromatic dispersion [19]

From (2), β_1 is associated to the group velocity and regulates the optical pulse envelope speed along the fiber:

$$\beta_1 = \frac{1}{v_G} = \frac{1}{c} \left(n + \omega \frac{dn}{d\omega} \right) \quad (5)$$

where ω is the optical frequency, n is the linear refractive index and c is the speed of light in vacuum. The broadening of a propagated pulse is caused by the group-velocity dispersion (GVD) coefficient β_2 which is given by:

$$\beta_2 = \frac{1}{c} \left(2 \frac{dn}{d\omega} + \omega \frac{d^2n}{d\omega^2} \right) \quad (6)$$

The dispersion component D is related to β_1 , and may be determined by calculating the first derivative of β_1 with regard to the wavelength:

$$D = \frac{d\beta_1}{d\lambda} = -\frac{2\pi c}{\lambda^2} \beta_2 \approx \frac{\lambda}{c} \frac{d^2n}{d\lambda^2} \quad (7)$$

$\beta_3 = d\beta_2/d\omega$ is the GVD slope factor, which corresponds to the dispersion slope parameter S :

$$S = \frac{d\beta_2}{d\omega} = -\frac{4\pi c^2}{\lambda^3} \beta_2 + \left(\frac{2\pi c}{\lambda^2} \right)^2 \beta_3 \quad (8)$$

The GVD slope becomes prominent and it must be accounted for the propagation in the region of zero dispersion ($\beta_2 = 0$). When a retarded time frame $T = t - z/v_G$ is introduced and travels with the signal at the group velocity, β_1 is removed from the equation. Moreover, the effect of the GVD slope can be ignored when SSMF or other types with high GVD are employed.

$$\frac{\partial A}{\partial z} + \frac{\alpha}{2} A + \frac{j}{2} \beta_2 \frac{\partial^2 A}{\partial T^2} = 0 \quad (9)$$

The waveguide dispersion D_W and the material dispersion D_M together define the overall dispersion profile. The combination of these two factors yields the dispersion profile in SSMF, which can be seen in Figure 4. At 1324 nm, the wavelength of zero dispersion exists, while at 1550 nm, $D=16$ ps/Km/nm [20].

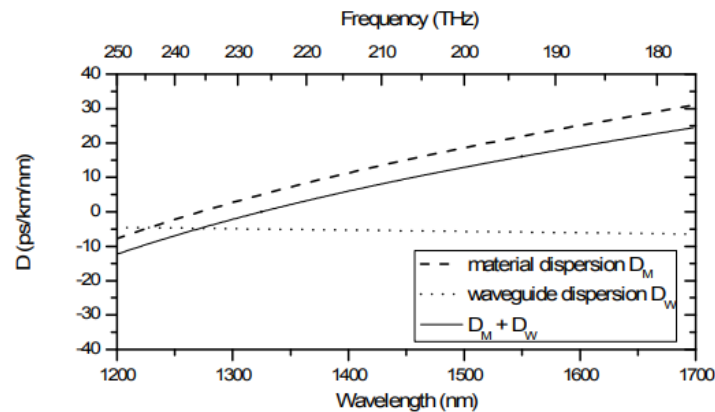


Figure 4. The dispersion of a typical SSMF as just a function of frequency and wavelength [16]

2.1.4. Polarization mode dispersion

The direction of the transverse electric field is indicated by the polarization of light, which is a property of electromagnetic waves. There are two orthogonal polarization cases in SMF: X and Y. The Stokes parameters can be used to identify the illustration of light polarization, which is easily expressed with the Poincaré sphere. As shown in Figure 5, this sphere is organized into four optical power specification [14].

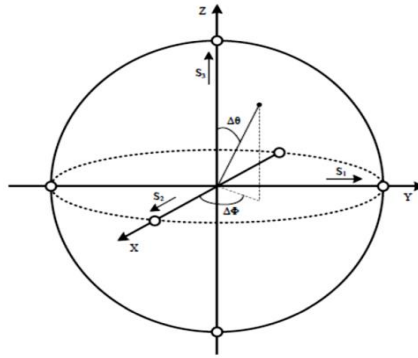


Figure 5. The sphere of Poincaré. Stocks parameters are $S_1, S_2,$ and S_3 [14]

SMF enable the propagation of two orthogonal polarization modes. Temperature changes and random birefringence caused by mechanical stress lead the states of polarization (SOP) and, as a result, GVD to fluctuate over time and over the entire length of the fiber. The SOP variation often happens on a length scale ranging from hundreds of meters to a few kilometers. Modal birefringence B_m , can be defined mathematically as:

$$B_m = \frac{|\beta_x - \beta_y|\lambda}{2\pi} = |n_x - n_y| \tag{10}$$

The effective refractive indexes of both modes are n_x and n_y , respectively, and the equivalent propagation constants are β_x and β_y . The fast axis is typically designated as the axis with the largest group velocity, while the slow axis is designated as the axis with the smallest group velocity [20]. Figure 6 shows a linearly polarized pulse that is released into a fiber at such a 45° angle towards the slow axis.



Figure 6. Random birefringence and the associated DGD for a wave delivered into the fiber at a 45° angle [16]

Differential group delay ΔT (DGD) is the difference between the arriving times of the two pulses, and it has a Maxwellian distribution around the mean DGD-value $\langle \Delta T \rangle$ [16].

$$\langle \Delta T \rangle = PMD \cdot \sqrt{L} \tag{11}$$

DGD is proportional to the square root of the transmission length L [21]. The pulse stream starts to overlap as the pulse spreading due to PMD expands, generating ISI, which decreases the BER performance [19].

2.2. Nonlinear impairments

At large data rate transmissions, nonlinear effects constitute a significant performance bottleneck. The Kerr effect, which results from the optical fiber's refractive index being dependent on the intensity of the transmitted signal, causes the optical fiber to be a nonlinear channel. Self-phase modulation (SPM), cross-phase modulation (XPM), and four wave mixing (FWM) are types of nonlinearities caused by this phenomenon. Nonlinear effects can also be induced through inelastic scattering, such as stimulated Brillouin scattering (SBS) and stimulated Raman scattering (SRS) [3]. One distinction between the scattering effect and the Kerr effect is that the scattering effect has a threshold power level above which nonlinear effects appear, whereas the Kerr effect does not [13]. Only above a threshold power density can Brillouin scattering become significant. It can be proved that the threshold power for SBS is given by:

$$P_{th} = 4.4 \times 10^{-3} d^2 \lambda^2 \alpha \nu \quad (\text{watts}) \quad (12)$$

Where λ and d are the operating wavelength and fiber core diameter in micrometers, respectively. α is the fiber attenuation in decibels per kilometer. The source bandwidth in gigahertz is denoted by ν [22]. In WDM channels, SRS causes a transfer of power from shorter wavelength channels to longer wavelength channels [23]. The optical power threshold for SRS is determined by:

$$P_{th} = 5.9 \times 10^{-2} d^2 \lambda \alpha \quad (\text{watts}) \quad (13)$$

Where d , λ and α are as specified for (12) above [24]. Decompose the optical field A in (9) into multiple interacting field components A_0 , A_1 , and A_2 , each expressing a separate WDM channel, with $\Delta\beta$ indicating the phase relationship among them. To demonstrate the impact of nonlinearity, confine the investigation to small signal distortions, and split (9) into three coupled equations, e.g. for A_0 [25]:

$$\frac{\partial A}{\partial z} + \frac{\alpha}{2} A + \frac{j}{2} \beta_2 \frac{\partial^2 A}{\partial T^2} = j\gamma |A_0|^2 A_0 + 2j\gamma (|A_1|^2 + |A_2|^2) A_0 + j\gamma \sum_{l,m \neq 0} A_l A_m A_{l+m}^* e^{j\Delta\beta z} \quad (14)$$

where $A(z, t)$ represents the slowly varying envelope related with the optical signal, α demonstrates fiber losses, β_2 determines GVD effects, and γ is the nonlinear component [26]. The linear phase mismatch is denoted by $\Delta\beta$. The SPM, XPM, and FWM have been described in (13), respectively, through the three right-hand portions [16].

3. METHODS AND RESULTS

3.1. Characterization of linear impairments

3.1.1. The impact of group velocity dispersion (GVD)

To illustrate the impact of GVD, the bit rate was set to 40 Gb/s as shown in Figure 7, corresponding to a bit duration of 25 ps. The pulse has an FWHM of 12.5 ps. When using the optical Gaussian pulse generator, the standard value for width is 0.5. The pulse width T_o parameter is then $T_o \approx \frac{T_{FWHM}}{1.665} = \frac{12.5 \text{ ps}}{1.665} = 7.5 \text{ ps}$. The dispersion length is calculated using the value of $\beta_2 \approx -20(\text{ps}^2)/\text{km}$ at $1.55\mu\text{m}$ for SMF: $L_D = \frac{T_o^2}{|\beta_2|} = \frac{(7.5)^2}{20} = 2.812 \text{ km}$.

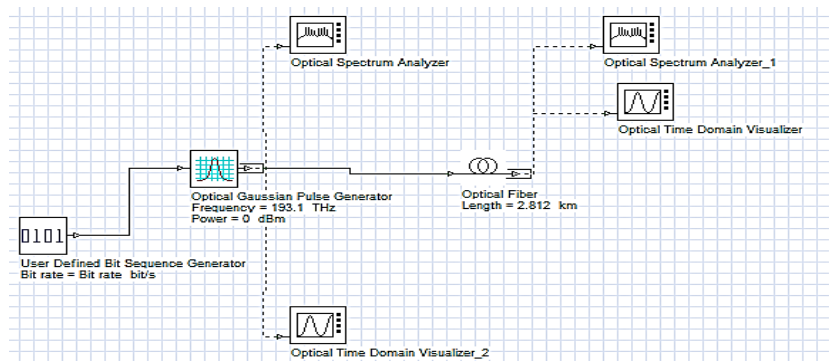


Figure 7. GVD system layout

Where $\beta_2 = \frac{\partial^2 \beta}{\partial \omega^2}$ is the GVD parameter, that is identified as the frequency-dependent second derivative of the fiber mode propagation constant. The pulse starts to broaden at this length (the peak power decreases). To demonstrate the effect of GVD on the optical Gaussian pulse, vary the fiber length between 2.812, 5, and 10 Km in the optical fiber properties, and disable all effects except GVD, with $\beta_2 = -20\text{ps}^2/\text{km}$. After that, take different GVD values, $\beta_2 = -20, -40, -60$ and $-80 \text{ ps}^2/\text{km}$, and different fiber lengths are considered to show the effect of GVD on the received power. Figure 8 illustrates received power versus fiber length for different GVD values. As shown in Figure 9 in time domain, after LD pulse start to broadening. With increasing fiber length, the peak power decreases and the pulse broadening can be observed due to group-velocity dispersion (GVD) coefficient.

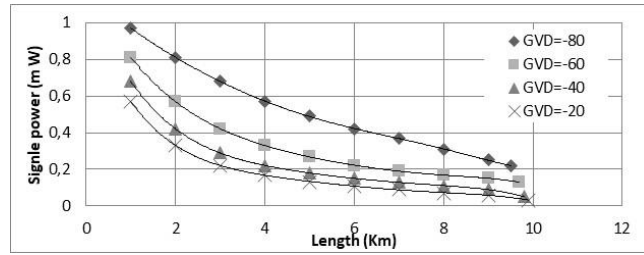


Figure 8. Received power vs. fiber length for different β_2

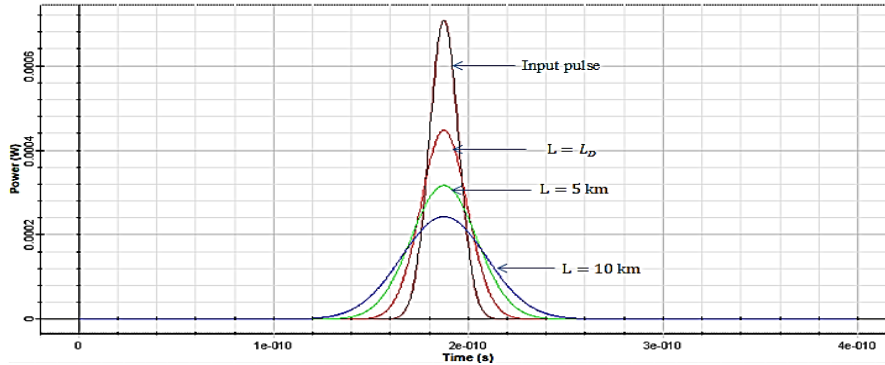


Figure 9. Broadening of optical gaussian pulse

3.1.2. The impact of polarization mode dispersion (PMD)

The PMD emulator is used to show signal distortions induced by PMD effects as shown in Figure 10. The system simulate a data rate of 10 Gb/s. The parameters of PMD emulator are shown in Table 1. Stokes vector and the poincare sphere have been applied to get the state of polarization (SOP).

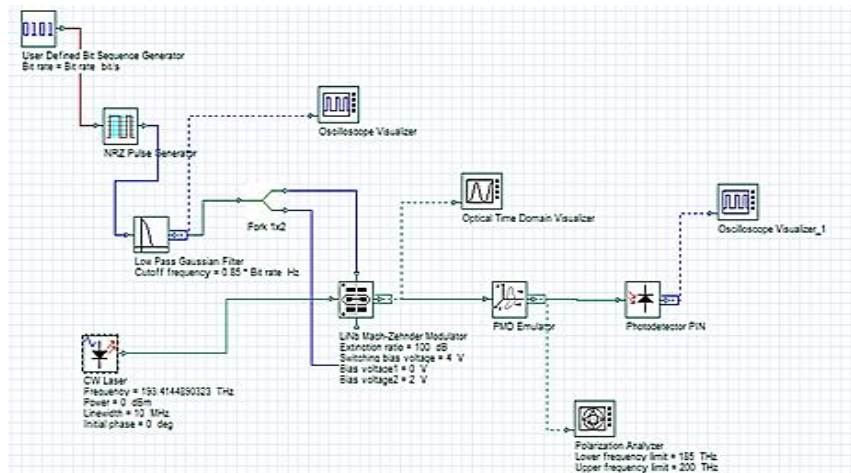


Figure 10. PMD system layout

Table 1. PMD emulator parameters

Parameter	Value
Length	10 Km
Attenuation	0 dB/Km
Dispersion	0 ps/(nm-km)
Dispersion slope	0 ps/(nm ² -km)
Frequency reference	193.414 THz
Differential Group Delay	71 ps
Depolarization rate	10.8 deg/GHz
Polarization chromatic dispersion	1.3 ps/GHz

The optical input signal is simulated in three different polarizations. The depolarization rate coefficient is responsible for the majority of the PMD effect. Figure 11 shows the SOP of the received signal, so Figure 11(a) shows the Poincare SOP graph when azimuth is 0° and ellipticity is 0°, Figure 11(b) shows the Poincare SOP graph when azimuth is 45° and ellipticity is 0°, and Figure 11(c) shows the Poincare SOP graph when azimuth is 90° and ellipticity is 0°. Figure 12 shows the Stokes vector of the received signal, with Figures 12(a) showing the Stokes vector of the output pulses for the state of polarization (SOP) azimuth 0° and ellipticity 0°, Figure 12(b) showing the SOP azimuth 45° and ellipticity 0°, and Figure 12(c) showing the SOP azimuth 90° and ellipticity 0°.

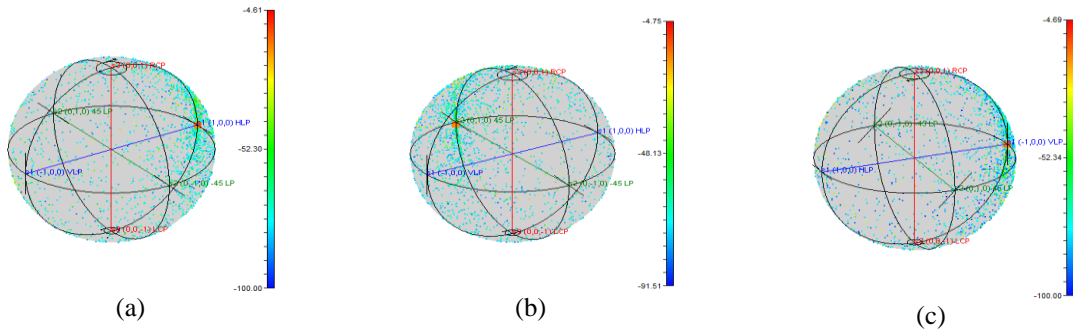


Figure 11. SOP of the received signal when the input signal: (a) azimuth 0° and ellipticity 0°, (b) azimuth 45° and ellipticity 0°, and (c) azimuth 90° and ellipticity 0°

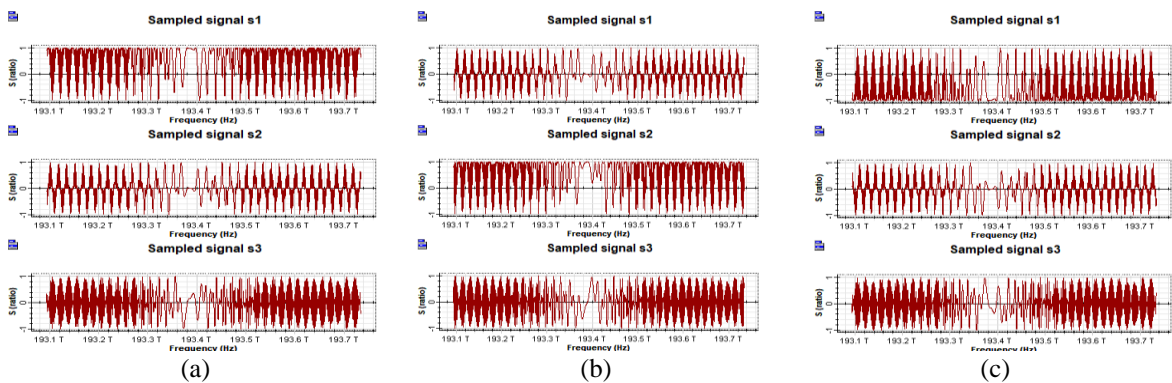


Figure 12. Stokes vector of the received signal when the input signal: (a) azimuth 0° and ellipticity 0°, (b) azimuth 45° and ellipticity 0°, and (c) azimuth 90° and ellipticity 0°

3.2. Characterization of nonlinear impairments

3.2.1. The impact of self phase modulation (SPM)

The following layout in Figure 13 can be used to show the effect of SPM: with a bit rate of 40 Gb/s, sequence length is 8 bits, sample per bit is 64, the number of samples is 512, and the reference wavelength is 1550nm. Disable all effects except SPM in the nonlinear dispersive fiber total field component characteristics. Set the transmission length to 10.73 Km.

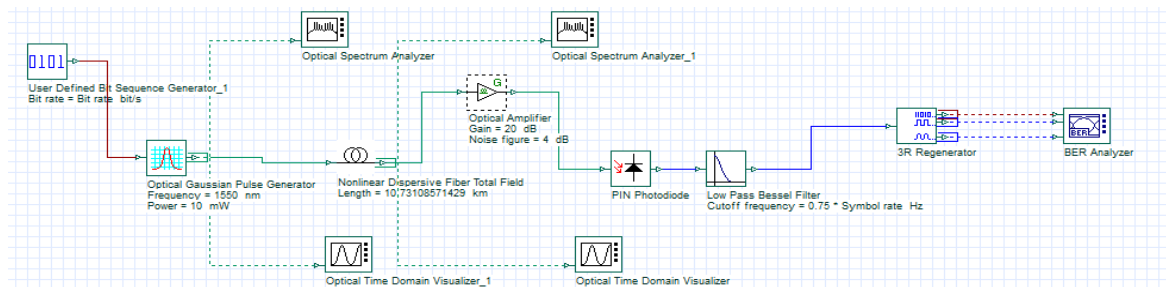


Figure 13. SPM system layout

The parameters of the nonlinear dispersive fiber total field are shown in Table 2, Figure 14 shows the input and output pulse shapes. Figure 14(a) shows the input pulse shape, and Figure 14(b) shows the output pulse shape after the Nonlinear Fiber. The nonlinear phase shift caused by SPM can be reduced by increasing the core effective area. Figure 15 shows this relationship in terms of the Q-factor.

Table 2. Nonlinear dispersive fiber parameters

Parameter	Value
Differential group delay (DGD)	0 ps/Km
Pulse peak power	From 0 to 20 dBm
Fiber nonlinearity coefficient (γ)	1.317 W ⁻¹ Km ⁻¹ 16.57 ps/nm-Km
Dispersion Effective area	40, 60 and 80 μm^2

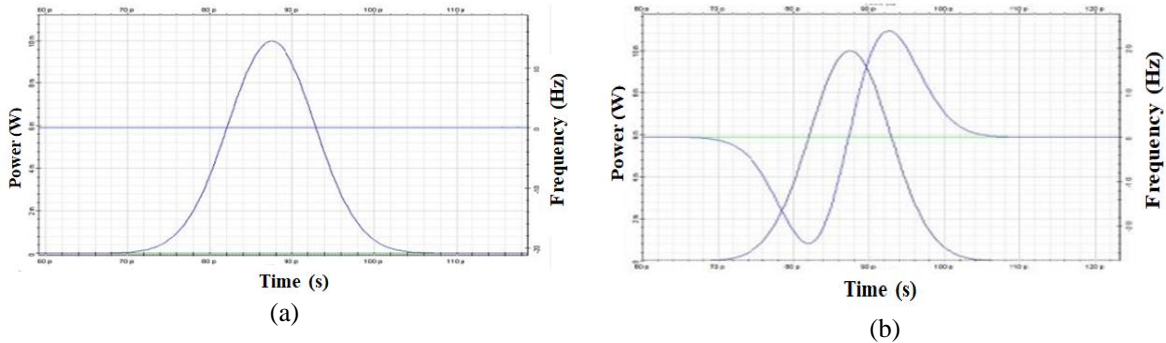


Figure 14. Pulse shapes: (a) prior and (b) following to the nonlinear dispersive fiber

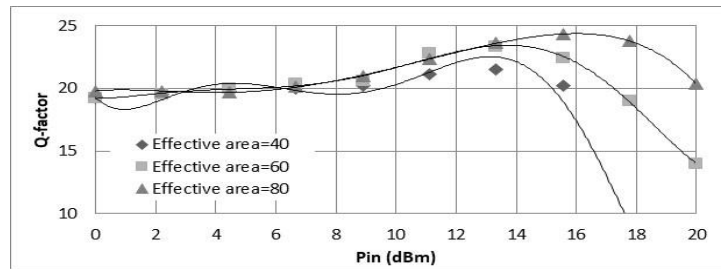


Figure 15. Q-factor increased by increasing core effective area

3.2.2. The impact of cross phase modulation (XPM)

The objective of this simulation is to provide an analysis of the impact of XPM in a nonlinear dispersive fiber at varied carrier frequencies with a bit rate of 2.5 Gbit/sec as shown in Figure 16. The input is comprised of two Gaussian pulses, weak and strong pulses separated by 800 ps in time and 1 nm in frequency. Figure 17 illustrates the input signals and their spectra. The peak power of the pulse at 1551 nm is 2 mW, and the peak power of the pulse at 1,550 nm is 20 mW.

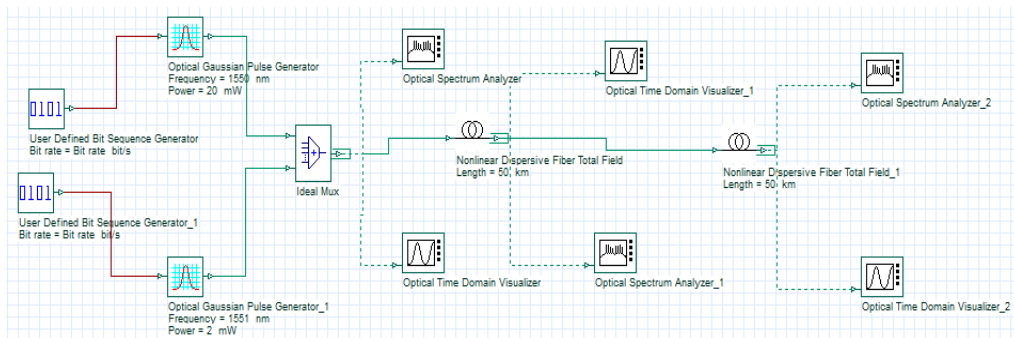


Figure 16. XPM system layout

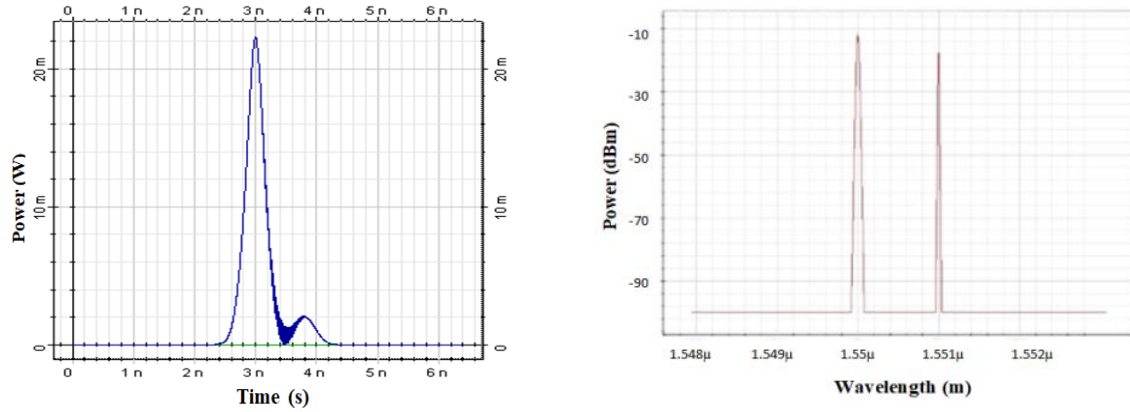


Figure 17. Input signals and their spectrums

The two pulses overlap after 50 Km of propagation as shown in Figure 18, broadening the spectrum of the pulse at 1551 nm, which is the result of the influence of XPM and is small due to the presence of GVD. The spectral broadening of the pulse at 1550 nm is greater, but this is due to SPM. When the pulses no longer overlap at 100 Km, the XPM-induced spectral broadening disappears as represented in Figure 19. This is because the impacts of increasing pulse overlap are diametrically opposed to those of increasing pulse separation.

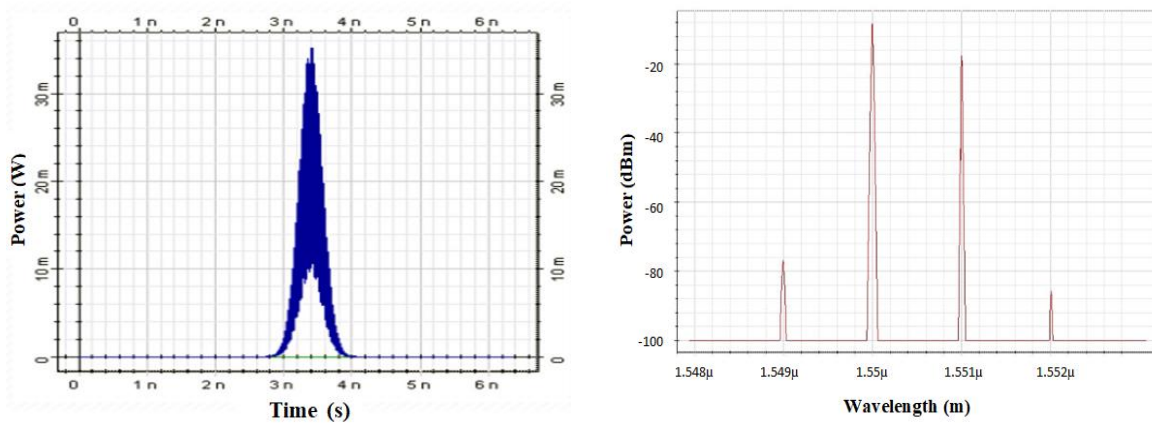


Figure 18. Signals and their spectrums after 50 Km of transmission

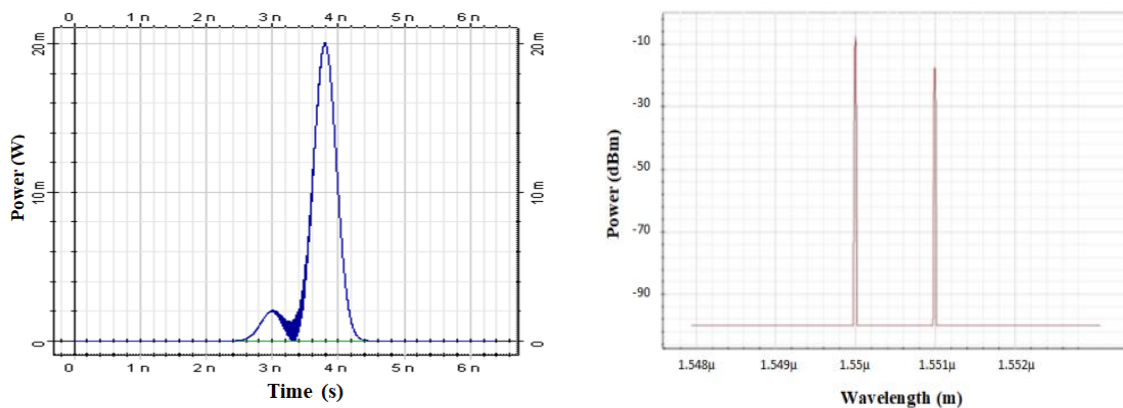


Figure 19. Signals and their spectrums after 100 Km of transmission

3.2.3. The impact of four wave mixing (FWM)

To determine how the FWM affects the optical fiber transmission link, two CW lasers with frequencies of 1540 and 1540.5 nm, a bit rate of 2.5 Gb/s, power of 0 dBm, and linewidth of 0 MHz are used as shown in Figure 20. Nonlinear fiber parameters are shown in Table 3. A 2x1 Mux was used to combine the channels. The signals are then sent along 75 Km of nonlinear fiber. Figure 21 displays the optical spectrums of two CW lasers. Figure 21(a) depicts the optical spectrums of two CW lasers before 75 Km of SMF, and Figure 21(b) shows the four-wave mixing products ("spurious frequencies") at 1539.5 nm and 1541 nm. After that, input power was changed to 13 dBm to demonstrate that with increasing launch power, Q-factor decreased due to the impact of FWM as shown in Figure 22.

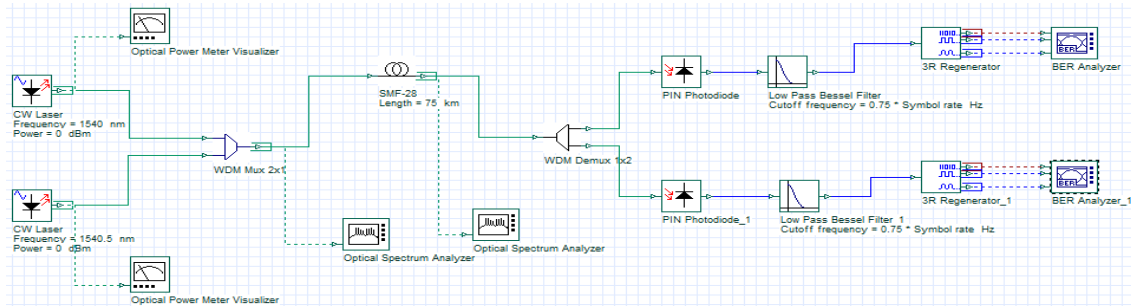


Figure 20. FWM system layout

Table 3. Nonlinear fiber parameters

Parameter	Value
Dispersion	1 ps/nm/Km
Dispersion slope	0.11 ps/nm ² /Km
Nonlinear index of refraction (n ₂)	4.3286 × 10 ⁻²¹ m ² /W
Max. nonlinear phase shift	3 mrad
Effective area	64 μm ²

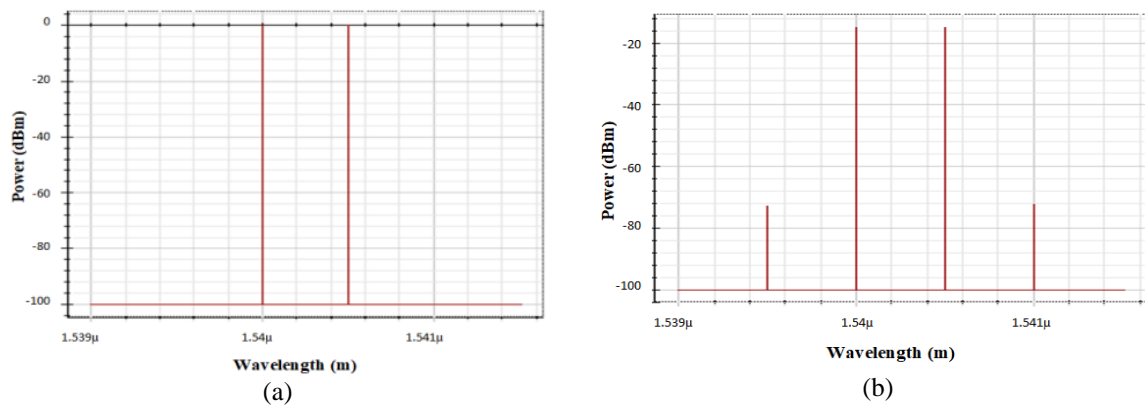


Figure 21. Optical spectrums of two CW lasers, (a) before SMF and (b) after SMF

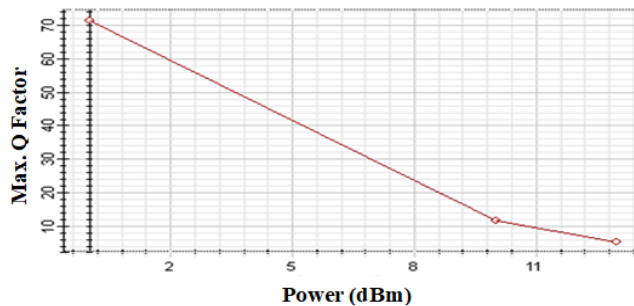


Figure 22. Q-factor vs input power




4. CONCLUSION

The impact of physical layer impairments on fiber optic channels was investigated using analytical modeling and validated using simulation results in this paper. It is demonstrated that linear and nonlinear effects in optical communication networks, like GVD, PMD, SPM, XPM, and FWM, constrain the network's transmission reach and capacity. The achievement of high-bit-rate long-distance optical transmission networks is determined by how well the linear and nonlinear impacts are handled. Therefore, when designing optical fiber communication systems, linear and nonlinear effects must be taken into account.




REFERENCES

- [1] F. F. B. Öncel, "Modulation formats for wavelength division multiplexing (WDM) systems," M.S. thesis, Dept. Physics, Middle East Technical Univ., Çankaya, Turkey, 2009.
- [2] T. Sabapathi and R. Poovitha, "Combating the effect of nonlinearities in DWDM system," *2017 4th International Conference on Electronics and Communication Systems (ICECS)*. IEEE, Feb. 2017, pp. 38–42, doi: 10.1109/ECS.2017.8067876.
- [3] G. Keiser, "Performance Impairments," in *Optical communications essentials*, USA : McGraw-Hill Education, Inc., 2003. ISBN 0-07-141204-2.
- [4] A. Y. Fattah and N. Q. Flaih, "Generation and transmission of optical solitons in ultrahigh speed long-haul systems," *Engineering & Technology Journal*, vol. 34, no. 7, pp. 1427–1436, 2016.
- [5] A. Y. Fattah and R. H. Abbas, "33% RZ-DPSK 10 Gb/s WDM transmission," *Engineering & Technology Journal*, vol. 29, no. 11, pp. 2282–2279, 2011.
- [6] M. Haris, "Advanced modulation formats for high-bit-rate optical networks," Ph.D. dissertation, Dept. Elect. and Comp. Eng., Georgia Institute of Technology, Atlanta, USA, 2008.
- [7] S. S. Husain, J. K. Hmood, and S. W. Harun, "Efficiency enhancement of phase-conjugated twin waves technique by shaping envelopes of subcarriers in all-optical OFDM systems," *Optics Communications*, vol. 472, pp. 1–7, Apr. 2020, doi: 10.1016/j.optcom.2020.125864.
- [8] J. S. Malhotra, M. Kumar, and A. K. Sharma, "Estimation and mitigation of FWM penalties in dispersion managed 32 channel long haul DWDM soliton link," *Optik*, vol. 124, no. 17, pp. 3029–3032, Sep. 2013, doi: 10.1016/j.ijleo.2012.09.050.
- [9] A. D. Ellis *et al.*, "The impact of phase conjugation on the nonlinear-Shannon limit: The difference between optical and electrical phase conjugation," *2015 IEEE Summer Topicals Meeting Series (SUM)*. IEEE, pp. 209–210, Jul. 2015, doi: 10.1109/PHOSST.2015.7248271.
- [10] R. Agalliu and M. Lucki, "Benefits and limits of modulation formats for optical communications," *Advances in Electrical and Electronic Engineering*, vol. 12, no. 2, pp. 160–167, Jun. 2014, doi: 10.15598/aece.v12i2.992.
- [11] J. K. Hmood, K. A. Noordin, H. Ahmad, and S. W. Harun, "Performance improvement of all-optical OFDM systems based on combining RZ coding with m-array QAM," *Journal of Optoelectronics and Advanced Materials*, vol. 17, no. 1–2, pp. 33–38, Feb. 2015.
- [12] A. Rouf and M. S. Islam, "A new approach of unequally spaced channel allocation for FWM crosstalk suppression in WDM transmission system," *2012 7th International Conference on Electrical and Computer Engineering*. IEEE, Dec. 2012, pp. 35–38, doi: 10.1109/ICECE.2012.6471478.
- [13] A. Y. Fattah and A. R. Farhan, "Spectral efficiency improvement of the optical communication systems," *Iraqi Journal of Computers, Communications, Control, and Systems Engineering*, vol. 14, no. 1, pp. 44–57, 2014.
- [14] S. Al-Awis and A. Y. Fattah, "Characterization of physical layer impairments impact on optical fiber transmission systems," *International Journal of Electronics and Communication Engineering and Technology*, vol. 7, no. 3, pp. 87–102, May–June 2016.
- [15] R. Rajana and K. Suresh, "Performance analysis of dispersion compensation using FBG and DCF in WDM systems," *International Journal of Engineering Technology Science and Research*, vol. 3, no. 10, pp. 5–9, 2016.
- [16] A. S. Abbas, "Mitigation of distortion in WDM systems based on optical phase conjugation," Ph.D. dissertation, Dept. Elec. and Comm. Eng., Univ. of Baghdad, Baghdad, Iraq, 2017.
- [17] A. GP, "Nonlinear Fiber Optics," Academic Press, Boston, MA, 1995.
- [18] S. L. Jansen, "Optical phase conjugation in fiber-optic transmission systems," *Dissertation Abstracts International*, vol. 68, no. 01., Eindhoven Univ. of Tech., Eindhoven, Netherlands, 2006, doi: 10.6100/IR610247.
- [19] N. Albakay, "Design and analysis of binary driven coherent m-ary qam transmitter for next generation optical networks," Ph.D. dissertation, Dept. Elect. and Comp. Eng., Univ. of Nebraska, Nebraska, USA, 2018, doi: 10.1109/JLT.2018.2863653.
- [20] C. Behrens, "Mitigation of nonlinear impairments for advanced optical modulation formats," Ph.D. dissertation, Dept. Elect. and Electron. Eng., Univ. College London, London, United Kingdom, 2012.
- [21] Saktioto *et al.*, "Birefringence and polarization mode dispersion phenomena of commercial optical fiber in telecommunication networks," *Journal of Physics: Conference Series*, IOP Publishing, vol. 1655, no. 1, Oct. 2020, p. 012160, doi: 10.1088/1742-6596/1655/1/012160.
- [22] J. M. Senior and M. Y. Jamro, "Transmission characteristics of optical fibers," in *Optical Fiber Communications Principles and Practice*, 3rd ed. Essex CM20 2JE, England : Pearson Education, 2009.
- [23] I. Rasheed, M. Abdullah, S. Mehmood, and M. Chaudhary, "Analyzing the non-linear effects at various power levels and channel counts on the performance of DWDM based optical fiber communication system," *2012 International Conference on Emerging Technologies*. IEEE, Oct. 2012, pp. 1–5, doi: 10.1109/ICET.2012.6375446.
- [24] T. Sabapathi and R. Poovitha, "Mitigation of nonlinearities in fiber optic DWDM system," *Optik*, vol. 185, pp. 657–664, May 2019, doi: 10.1016/j.ijleo.2019.02.073.
- [25] P. J. Winzer and R. J. Essiambre, "Advanced optical modulation formats," *Proceedings of the IEEE*, vol. 94, no. 5, May 2006, pp. 952–985, doi: 10.1109/JPROC.2006.873438.
- [26] P. L. Christiansen, M. P. Sorensen, and A. C. Scott, *Nonlinear Science at the Dawn of the 21st Century*, Lecture Notes in Physics, vol. 542. Berlin, Germany : Springer Science & Business Media, 2000, doi: 10.1007/3-540-46629-0.




BIOGRAPHIES OF AUTHORS

Riyam Saadi Ali    was born in Baghdad, Iraq in 1991. She received a Bachelor's degree in Electronics and Communication Engineering from University of Baghdad, Iraq in 2013. She is currently studying toward a Master's degree of Science in Optical Communications Engineering at the University of Technology, Iraq. She can be contacted at email: coe.20.02@grad.uotechnology.edu.iq.



Assistant Professor Dr. Ali Y. Fattah    was born in Iraq, 1960. He earned his Ph.D. in Electrical Engineering from the Department of Theoretical Principles of Electrical Engineering at Saint Petersburg State Technical University, Russia, 1991. And he earned his bachelor's degree in electrical engineering from the University of Baghdad, Iraq in 1982. He is a faculty staff member in the Electrical & Communication Engineering Departments at the University of Technology (UOT) of Baghdad since 1992. His research interested focus on Optical Fiber Communications and Optical Networks. He can be contacted at email: ali.y.fattah@uotechnology.edu.iq.



Mustafa D. Hassib    was born in Baghdad, Iraq. He received his bachelor's degree in Electronics and Communications Engineering from the University of Technology Iraq, in 1991 and his master's degree in Communications Engineering from the Military Engineering college at Baghdad, Iraq in 2004 and the Ph.D. degree in mobile wireless communications from the National University of Malaysia (UKM), in 2015. He has held various positions in the Department of communications at the University of Technology Iraq. His research interests take account of mobile wireless communication, Optical communication and coding theory. He can be contacted at email: mustafa.d.hassib@uotechnology.edu.iq.